Glycobiology vol. 23 no. 12 pp. 1531–1546, 2013
doi:10.1093/glycob/cwt085
Advance Access publication on October 2, 2013

N-/O-glycosylation analysis of human FVIIa produced in the milk of transgenic rabbits

Guillaume Chevreux[1,2], Valegh Faid[2], Jean-Marc Scohyers[2], and Nicolas Bihoreau[2]

[2]Analytical Department, LFB Biotechnologies, 3 Avenue des Tropiques, Les Ulis, 91942 Courtaboeuf, France

Received on July 5, 2013; revised on September 18, 2013; accepted on September 20, 2013

Human coagulation factor VIIa is a glycoprotein that promotes haemostasis through activation of the coagulation cascade extrinsic pathway. Most haemophilia A/B patients with inhibitors are treated by injection of plasma-derived or recombinant FVIIa. The use of recombinant products raises questions about the ability of the host cell to produce efficiently post-translationally modified proteins. Glycosylation is especially critical considering that it can modulate protein safety and efficacy. The present paper reports the N-/O-glycosylation pattern of a new recombinant human factor VIIa expressed in the mammary glands of transgenic rabbits. Glycosylation was investigated by chromatography and advanced mass spectrometry techniques for glycan identification and quantitation. Mass spectrometry (MS)/MS analyses were performed to confirm the glycan structures as well as the position and branching of specific monosaccharides or substituents. The two N-glycosylation sites were found to be fully occupied mostly by mono- and bi-sialylated biantennary complex-type structures, the major form being $A_2G_2S_1$. Some oligomannose/hybrid structures were retrieved in lower abundance, the major ones being GlcNAcα1,O-phosphorylated at the C6-position of a Man residue (Man-6-(GlcNAcα1,O-) phosphate motif) as commonly observed on lysosomal proteins. No immunogenic glycotopes such as Galili (Galα1,3Gal) and HD antigens (N-glycolylneuraminic acid (NeuGc)) were detected. Con-cerning O-glycosylation, the product exhibited O-fucose and O-glucose-$(xylose)_{0,\ 1,\ 2}$ motifs as expected. The N-glycosylation consistency was also investigated by varying production parameters such as the period of lactation, the number of consecutive lactations and rabbit generations. Results show that the transgenesis technology is suitable for the long-term production of rhFVIIa with a reproducible glycosylation pattern.

Keywords: coagulation factor VII / glycosylation / mass spectrometry / transgenic

Introduction

Human coagulation factor VII is a vitamin K-dependent glycoprotein that participates, under its activated form, in the coagulation cascade through the activation of factors X and IX (FX and FIX). The protein is composed of an N-terminal Gla domain that contains 10 modified Gla residues, followed by two epidermal growth factor domains and a C-terminal protease domain. Human FVII is also β-hydroxylated at Asp_{63}, O-glycosylated at both Ser_{52} and Ser_{60} and N-glycosylated at both Asn_{145} and Asn_{322} (Hansson and Stenflo 2005). Its activated form (hFVIIa) is used to control bleeding episodes in patients affected by haemophilia A or B with circulating inhibitory antibodies against FVIII or FIX (Brinkhous et al. 1989; Lusher et al. 1998). Currently, the available sources of hFVIIa either come from plasma concentrates (Tomokiyo et al. 2003) or are derived from the recombinant technology (Hedner and Lee 2011). Today, the only recombinant human FVIIa (rhFVIIa) available is NovoSeven® (rhFVIIa; Eptacog alfa; Novo Nordisk, Copenhagen, Denmark), which is produced in baby hamster kidney (BHK) cells that are cultured in the presence of newborn calf serum. However, this production system has low expression levels that result in high end-user costs, making the preferred product cost-prohibitive for some of the potential new clinical indications. Therefore, an alternative production source of rhFVIIa at lower cost with easily expandable manufacturing capacity is necessary to cover the increasing patient needs.

During the last few years, the production of proteins in transgenic animals using a milk protein gene promoter to drive specific expression of the gene coding for the protein of interest has gained much attention (Van Cott and Velander 1998). This strategy offers several advantages: The protein can be recovered easily by milking the animals and large amounts of product can be harvested at low cost. As a consequence, biopharmaceutical production from the milk of transgenic animals can often overcome problems of low yields and production scale-up issues associated with current mammalian cells used for expression of post-translationally modified complex proteins. So far, Atryn®, a human antithrombin III produced by transgenic goats, and Ruconest®, a human C1 inhibitor (rhC1INH) produced by transgenic rabbits, are the only transgenic recombinant products approved on the market, respectively, for the prevention of perioperative/peri-partum thromboembolic events in hereditary antithrombin deficiency and for the treatment of patients with hereditary angioedema (Menache et al. 1992; Carugati et al. 2001).

[1]To whom correspondence should be addressed: Tel: +33-1-69-82-73-37; Fax: +33-1-69-82-56-55; e-mail: chevreuxg@lfb.fr; g.chevreux@wanadoo.fr

One of the most important challenges when dealing with the bioproduction of complex proteins is to generate a molecule exhibiting appropriate post-translational modifications (PTMs). N-glycosylation is of great importance for biomanufacturers as this PTM often influences many of the protein properties such as stability, bioactivity, plasma half-life and immunogenicity (Varki 1993). To warrant the safety and efficacy of a biopharmaceutical product, its N-glycosylation profile has to be determined and attested to be consistent.

However, N-glycosylation is particularly known to be heterogeneous and strongly dependent on various parameters, which makes it difficult to reproduce. Indeed, N-glycosylation varies according to specific protein sequences; it is also tissue and species dependent and sensitive to the environment (culture conditions, temperature etc.). So far, N-glycosylation profiles of different proteins produced by the mammary gland of cows, goats, pigs and rabbits have been published. Human lactoferrin from cows has been described to contain some oligomannose and hybrid structures in addition to complex structures, which were the only type detected for the natural product (van Berkel et al. 2002). Complex-type N-glycans with some GalNAc instead of Gal residues at the nonreducing end of antennae (LacdiNAc) were also reported in this study. Both human erythropoietin (EPO) (Montesino et al. 2008) and antihrombin (Edmunds et al. 1998) expressed in goats were shown to contain mainly complex-type N-glycans with some LacdiNAc epitopes as well as NeuGc. Human coagulation factor IX produced by pigs (Gil et al. 2008) was described to contain major complex structures, some of them being sulfated or also bearing the LacdiNAc epitopes. Human C1-inhibitor (Koles et al. 2004a) and acid α-glucosidase (Jongen et al. 2007) expressed by rabbits share a glycosylation pattern composed of oligomannose, hybrid and complex-type structures. Neither LacdiNAc nor NeuGc has been reported for these two recombinant proteins. Some GlcNAc-1,O-phosphorylated oligomannosidic structures were evidenced, but only for the acid α-glucosidase. The presence of these GlcNAc-1,O-phosphorylated oligomannosidic structures was discussed regarding the fact that it could be specific to lysosomal enzymes. Finally, the glycosylation consistency of transgenic-derived proteins has only been investigated for the human C1-inhibitor (Koles et al. 2004b). In their study, the authors demonstrated that some variability occurs from rabbit to rabbit but by pooling the milk from multiple rabbits, they obtained batches with reproducible glycosylation profiles. They also found that protein glycosylation was evolving during lactation, i.e., the fucosylation, sialylation levels and oligomannose/hybrid content were decreasing as a function of the time of lactation. Finally, this latest study suggested for the first time that transgenic rabbits can be used to produce a protein suitable for human use with high robustness.

In this study, mass spectrometry (MS) was used to investigate the N-/O-glycosylation of a new rhFVIIa, specifically expressed by the mammary gland of transgenic rabbits via the control of a β-casein promoter and currently under clinical trial. Additionally, investigations were carried out to demonstrate the ability to consistently produce batches with reproducible N-glycosylation patterns. For this purpose, the breeding of successive generations, the effect of consecutive lactations and the evolution of the glycosylation profile during the lactation period were investigated.

Results

Sodium dodecyl sulfate–polyacrylamide gel electrophoresis analysis of rhFVIIa

RhFVIIa originating from a representative pilot batch has been used for structural characterization. Briefly, rhFVIIa has been produced in the mammary gland of lactating rabbits under the control of a β-casein promoter and purified using four chromatographic steps, the first one being an immunoaffinity step. The final product, deriving from the purification process at the 15 L manufacturing scale, reached high purity with host cell protein level measured in the low ppm range. The rhFVIIa N-glycans were completely released after peptide-N_4-(N-acetyl-beta-glucosaminyl)asparagine amidase (PNGase F) digestion, as determined by sodium dodecyl sulfate–polyacrylamide gel electrophoresis (SDS–PAGE). Under nonreducing conditions, native rhFVIIa migrates as a single sharp 47 kDa band, whereas after PNGase F digestion, it migrates at 43 kDa (see Figure 1A). The mass difference of 4 kDa is consistent with N-deglycosylation of the two Asn-X-Ser/Thr sites, as predicted from the sequence. The protein, also submitted to endo-β-N-acetylglucosaminidase H digestion (EndoH), showed to be partially sensitive to this enzyme with the emergence of one intermediate band at 45 kDa, indicating the loss of one N-glycosylation and one very minor band at 43 kDa, suggesting the loss of two N-glycosylation (see Figure 1A). This experiment indicates the presence of complex as well as oligomannose/hybrid structures. Under reducing conditions (see Figure 1B), the native protein exhibits two bands at 32 and 25 kDa, attributed respectively to glycosylated heavy and light chains. After PNGase F digestion, these two bands were retrieved at 29 and 21 kDa, respectively, indicating the full deglycosylation of each chain. EndoH digestion revealed a partial loss of the heavy chain glycosylation with the appearance of a band at 29 kDa and almost no deglycosylation of the light chain that remains at 21 kDa. This result indicates that oligomannose/hybrid structures should be localized preferentially on the rhFVIIa heavy chain.

Sialic-acid analysis of rhFVIIa N-glycans

Sialic-acid analysis after 1,2-diamino-4,5-methylenedioxybenzene (DMB) derivatization of sialic acids released under acidic conditions (see Figure 2) indicated the major presence of N-acetylneuraminic acid (NeuAc; 96.4%), trace amounts of NeuGc (0.4%) and a low content of N-acetyl-9-O-acetylneuraminic acid (2.4%).

Compositional analysis and quantitation using HILIC/FD and ESI-MS of 2-aminobenzamide labeled structures

The PNGase F-released N-glycans from rhFVIIa were analyzed after 2-aminobenzamide (2-AB) labeling, using hydrophilic interaction liquid chromatography (HILIC) for quantitation and compositional analysis by MS. Isolated fractions collected from HILIC were also investigated by MS using an offline nanoelectrospray ionization (nano-ESI) ion source and an

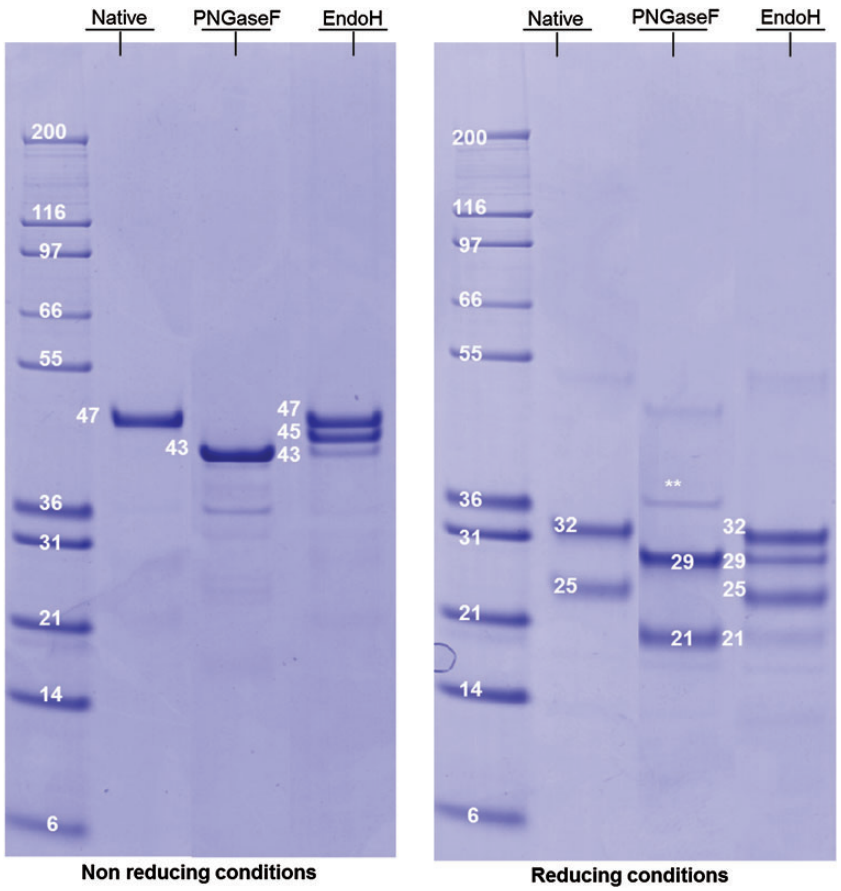

Fig. 1. SDS–PAGE profile of rhFVIIa derived from transgenic rabbits. The SDS–PAGE was performed under both nonreducing (left panel) and reducing conditions (right panel); rhFVIIa was analyzed in its native form (Lane 2), after PNGase F digestion (Lane 3), after EndoH digestion (Lane 4). The molecular weights are indicated in kDa.

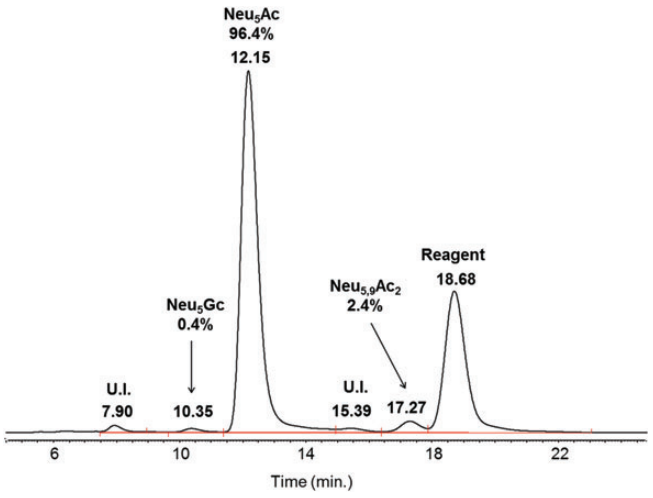

Fig. 2. Sialic-acid analysis of rhFVIIa DMB-labeled sialic acids; Neu5Ac was almost the only one detected at RT 12.15 min; U.I., unidentified.

Orbitrap mass spectrometer giving mass accuracies better than 5 ppm. The initial pool of derived glycans was also analyzed online on a reduced diameter HILIC capillary column coupled to an Orbitrap via the standard ESI ion source. Carbohydrate compositions were deduced by comparison of experimental with theoretical masses generated by the Glycoworkbench tool software. Sequencing information on each 2-AB-labeled structure was also used to confirm carbohydrate compositions, using fragments originating from the nonreducing part of glycans that are strong indicators of the glycan type, and also to drive hypothesis on putative structures, based on the current knowledge of mammalian N-glycan biosynthesis (Kamerling and Boons 2007). The fluorescence signal was used for quantification and retention times (RTs) measured from HILIC were used to point out the presence of additional isobaric positional isomers as well as to confirm identifications (using RTs of standard structures). A proposed carbohydrate composition is summarized in Table I.

MS signals detected at *m/z* 1234.4844[$^{+1}$] and 881.3380[$^{+2}$] correspond to neutral complex structures, the first mass corresponding to a structure commonly designated as A_1G_0, the nonreducing GlcNAc being probably on the Manα1,3 arm, according to the branch specificity of the β1,2-N-acetylglucosaminyltransferase I (Vella et al. 1984). The mass detected at *m/z* 881.3380[$^{+2}$] is consistent with a fully galactosylated structure (A_2G_2). These neutral complex structures represent <2% of the total N-glycan pool.

Table I. Monosaccharide composition of 2-AB labeled N-glycans from rhFVIIa, deduced from ESI-MS and LC-ESI-MS data analysis

Chromatographic data		Detected masses				Monosaccharide composition					Glycan name
RT (min)	Relative amount (%)	Experimental *m/z*	Theoretical *m/z*	Adduct	Deviation (ppm)	Hex	HexNAc	dHex	NeuAc	*P*-value	
30.9	0.7	1234.4844	1234.4832	$[M+1H]^{+1}$	−1.0	3	3	0	0	0	A_1G_0
43.7	1.5	1355.51	1355.5094	$[M+1H]^{+1}$	−0.4	5	2	0	0	0	Man_5
49.8	0.3	1558.5894	1558.5888	$[M+1H]^{+1}$	−0.4	5	3	0	0	0	$Man_4A_1G_1$
54.9	1.4	844.3196	844.3193	$[M+2H]^{+2}$	−0.4	4	3	0	1	0	$A_1G_1S_1$
57.7	1.1	881.338	881.3377	$[M+2H]^{+2}$	−0.3	5	4	0	0	0	A_2G_2
61.3	0.6	945.8601	945.859	$[M+2H]^{+2}$	−1.2	4	4	0	1	0	$A_2G_1S_1$
65.3	1.6	925.3457	925.3457	$[M+2H]^{+2}$	0.0	5	3	0	1	0	$Man_4A_1G_1S_1$
66.1–67.8	10.9	900.8075	900.8076	$[M+2H]^{+2}$	0.1	6	3	0	0	1	Man_6-P-GlcNAc
72.3	43.1	1026.8854	1026.8854	$[M+2H]^{+2}$	0.0	5	4	0	1	0	$A_2G_2S_1$
74.1–77.0	2.9	1006.3725	1006.3721	$[M+2H]^{+2}$	−0.4	6	3	0	1	0	$Man_5A_1G_1S_1$
78.3	7.0	1099.9142	1099.9144	$[M+2H]^{+2}$	0.2	5	4	1	1	0	$A_2G_2S_1F_p$
78.9	3.6	981.8341	981.834	$[M+2H]^{+2}$	−0.1	7	3	0	0	1	Man_7-P-GlcNAc
83.5	3.6	1099.9148	1099.9144	$[M+2H]^{+2}$	−0.4	5	4	1	1	0	$A_2G_2S_1F_d$
87.0	9.4	1172.4335	1172.4331	$[M+2H]^{+2}$	−0.3	5	4	0	2	0	$A_2G_2S_2$
89.2	2.0	1172.9404	1172.9433	$[M+2H]^{+2}$	2.5	5	4	2	1	0	$A_2G_2S_1F_pF_d$
91.3	3.0	1123.3574	1123.3568	$[M+2H]^{+2}$	−0.5	7	4	0	0	2	Man_7-(P-GlcNAc)$_2$
92.6	2.6	1245.4624	1245.4621	$[M+2H]^{+2}$	−0.2	5	4	1	2	0	$A_2G_2S_2F_p$
98.9	4.7	1228.9224	1228.9214	$[M+2H]^{+2}$	−0.8	7	4	0	1	1	Man_6-P-GlcNAc-$A_1G_1S_1$

Relative abundances (%) were deduced from integration of fluorescence signals recorded after HILIC chromatography.

Glycans at *m/z* 844.3196[$^{+2}$], 945.8601[$^{+2}$], 1026.8854[$^{+2}$], 1099.9142[$^{+2}$], 1172.4335[$^{+2}$], 1172.9404[$^{+2}$] and 1245.4624[$^{+2}$] correspond to complex sialylated structures accounting for 69% of the total N-glycan pool. Indeed, all of these ions display a strong fragment signal on their ESI-MS/MS mass spectra at *m/z* 657.23, indicating sialylated NeuAc-Hex-HexNAc antenna (data not shown). Signals at *m/z* 844.3196[$^{+2}$] and 945.8601[$^{+2}$] are consistent with complex structures having a sialylated antenna, probably on their Manα1,3 arm and a free core mannose on the Manα1,6 arm ($A_1G_1S_1$) or linked to an additional β1,2GlcNAc ($A_2G_1S_1$), respectively. The signal at *m/z* 1026.8854[$^{+2}$] has a composition consistent with a biantennary monosialylated structure ($A_2G_2S_1$). It is by far the major form detected having an abundance of 43.1% (see Table I). The signal at *m/z* 1099.9142[$^{+2}$] has a composition consistent with a biantennary monosialylated fucosylated glycan ($A_2G_2S_1F$), and this mass was retrieved at both RT 78.3 and 83.5 min (see Table I), which is explained by the presence of two isomers corresponding probably to α1-6 proximal and α1-3 distal fucosylation. The signal at *m/z* 1172.9404[$^{+2}$] is consistent with a bi-fucosylated monosialylated glycan ($A_2G_2S_1F_pF_d$), hence confirming the presence of distally fucosylated structures. The signals at *m/z* 1172.4335[$^{+2}$] and 1245.4624[$^{+2}$] are consistent with biantennary fully sialylated structures, the second one having an additional proximal fucosylation ($A_2G_2S_2$ and $A_2G_2S_2F_p$).

The masses detected at *m/z* 1355.5100[$^{+1}$], 900.8075[$^{+2}$], 981.8341[$^{+2}$] and 1123.3574[$^{+2}$] represent glycans of the oligomannose type and account for 19% of the total N-glycan pool. The first mass, consistent with a composition of the $Hex_5HexNAc_2$ type, corresponds to a Man_5 structure. The signal at *m/z* value of 900.8075[$^{+2}$] is consistent with a composition of the Hex_6-P-$HexNAc_3$ type (+0.1 ppm). The spectrum of this structure after MS/MS analysis (see Supplementary data, S1A) was used to support composition assignment. It showed the preferential loss of one N-acetylhexosamine (*m/z* 1597.53) and the sequential loss of six hexoses and a phosphate up to *m/z* 545.24 that corresponds to the two GlcNAc residues of the core. The mass difference of 79.969 Da between the fragments at *m/z* 1111.370 and 1031.401 confirmed a better match with a phosphorylation, giving a mass error of 3 mDa, instead of a sulfation that would give a mass error of 13 mDa. Fragment ion observed at *m/z* 405.08 corresponding to Hex_2-P can be used as a useful diagnostic ion of mannose-linked phosphate motif. Together, these data suggested a hexamannosidic structure with a Man-6-(GlcNAcα1,O-)phosphate element linked to a mannose residue (Man_6-P-GlcNAc). This structure was retrieved at both RT 66.1 and 67.8 min (see Table I), confirming the presence of two isomer structures. Similarly, a signal at *m/z* value of 981.8341[$^{+2}$] was detected and consistent with an oligomannosidic type structure containing also a Man-6-(GlcNAcα1,O-)phosphate element but having one additional mannose comparing with the previous one (Man_7-P-GlcNAc). At last, the signal at *m/z* 1123.3574[$^{+2}$] was consistent with an oligomannose structure containing two Man-6-(GlcNAcα1,O-)phosphate elements and seven mannose residues (Man_7-(P-GlcNAc)$_2$).

The signals observed at *m/z* values of 1558.5894[$^{+1}$], 925.3457[$^{+2}$], 1006.3725[$^{+2}$] and 1228.9224[$^{+2}$] correspond to hybrid glycans and accounted for ~10% of the total N-glycan pool. The ion at *m/z* 1558.5894[$^{+1}$] corresponds to a structure having one nonsialylated antenna on its Manα1,3 arm and one additional mannose on its Manα1,6 arm ($Man_4A_1G_1$). Ions at *m/z* values of 925.3457[$^{+2}$] and 1006.3725[$^{+2}$] have compositions consistent with structures having one sialylated antenna and respectively one and two additional mannose residues ($Man_4A_1G_1S_1$ and $Man_5A_1G_1S_1$). It should be noticed that the first hybrid structure was found to co-elute partially with an

oligomannose one at RT 65.3 (see Table I). Its relative abundance was approximated by integration of the peak shoulder. The relative abundances of $Man_4A_1G_1S_1$ and $Man_5A_1G_1S_1$ structures deduced from chromatography were in good accordance with results from matrix assisted laser desorption ionisation (MALDI) profiling of the permethylated structures (data not shown), assuming similar ionization for these two structures. The ion at *m/z* 1228.9224[$^{+2}$] was found consistent with a structure of the hybrid type composed of a core structure having a sialylated antenna, six additional mannose residues and a Man-6-(GlcNAcα1,O-)phosphate element (Man_6-P-GlcNAc-$A_1G_1S_1$). Its product ion profile obtained after ESI-MS/MS was used to support the compositional analysis (see Supplementary data, 1B) and showed the preferential loss of one N-acetylhexosamine (*m/z* 1127.38^{2+}), the presence of a fragment of Hex_6-P-$HexNAc_3$ composition having lost its sialylated antenna at *m/z* 1800.59, accompanied by fragments resulting from multiple losses (*m/z* 1597.53 and 1435.48) and diagnostic ion of complex sialylated antennae at *m/z* 657.23.

Finally, a detailed inspection of the set of registered product ion profiles enabled us to confirm the absence of fragment ions corresponding to antennae sialylated by NeuGc or having a LacdiNAc motif (respectively, *m/z* 673.23 or 698.26). Immunogenic Galα1,3Gal epitopes were not evidenced. The N-glycan pool was also found to be insensitive to a sialidase from *Macrobdella decora* that specifically cleaves α2,3-linked sialic acids (data not shown). This result indicates that sialic acids are exclusively bound in the α2,6-linkage type.

Further structural investigation by MS/MS of the permethylated N-linked oligosaccharides

Further structural details like the position and linkage of some glycan substituents were obtained by fragmentation of the permethylated structures, using an electrospray Orbitrap mass spectrometer and high-energy collisional dissociation (HCD) fragmentation. Uncertain structures, as well as the major precursor ions, were sequenced in this way. The MS/MS mass spectra of three structures of interest are described below.

Figure 3A shows the MS/MS product ion profile of the major N-glycan, which is a complex-type monosialylated biantennary structure detected as a doubly sodiated, doubly charged species at *m/z* 1227.0913^{2+}. The profile is mainly dominated by Y-type fragment ions, resulting from single and multiple loss(es) of nonreducing fragments mainly at HexNAc (see *m/z* 1967.95, 1606.78, 1592.76 and 1143.54) and at NeuAc residues (see *m/z* 2056.00, 1778.85, 1592.76 and 1388.67). B-type ions, resulting from loss(es) of reducing fragments, were also generated, mainly from the glycosidic bond cleavages at HexNAc (see *m/z* 486.23 and 847.40) and are particularly informative about the composition/structure of both antennae. The ion at *m/z* 847.40 is consistent with a sialylated LacNAc antenna, as confirmed by the subsequent loss of the nonreducing NeuAc (Y-type cleavage) to generate an internal fragment at *m/z* 472.21. The ion at *m/z* 486.23 indicated that the other antenna is a fully methylated (nonsubstituted) LacNAc unit. Two structurally relevant cross-ring cleavages derived from cleavages at the branching β-Man of the N-glycan core were observed at *m/z* 750.35 ($^{0,4}A_3$) and 778.38 ($^{3,5}A_3$), in agreement with a positioning of the nonsialylated LacNAc antenna onto the Manα1,6 arm, and thereby the sialylated LacNAc antenna onto the Manα1,3 arm. Furthermore, a putative position of the sialic acid onto the Manα1,6 arm is not supported by the presence of *m/z* 764.36 ($^{1,3}A_3$ or $^{2,4}A_3$). This result is in agreement with the branch specificity of the α2,6-sialyltransferase, which prefers to transfer NeuAc onto the Manα1,3 arm (Joziasse et al. 1985).

To determine the type of antenna (Type 1 vs. Type 2) as well as the nature of the sialyl linkage, MS^n fragmentations were carried out on protonated species, as described previously (Viseux et al. 1997; Morelle et al. 2004). Briefly, fragmentation of protonated molecular species produces predictable and intense antenna-relative oxonium ions, formed by cleavage of glycosidic bonds at HexNAc residues. When selected for a third-stage CID fragmentation, oxonium ions further fragment into intense secondary fragment ions resulting from the elimination of the three-linked substituents from HexNAc residues. In the case of rhFVIIa N-glycans, MS^3 product ion profiles of oxonium ions at *m/z* 825.42 (NeuAc-Gal-GlcNAc B-type ion) are dominated by an intense E-ion at *m/z* 793.40, which corresponds to a complete sialylated antenna-relative oxonium-derived conjugated diene, resulting from a β-elimination of the three-linked methoxy group (see Supplementary data, 2A). This result is indicative of Type 2 antenna with β1-4 linked galactose residues. Moreover, the relative intensities of the three main product ions (*m/z* 344.17, 580.30 and 793.40) consist of a typical spectral signature indicative of α2,6-sialyl linkage on the sequenced antenna, in agreement with the resistance of rhFVIIa N-glycans structures to the *M. decora* sialidase previously described.

Figure 3B depicts the MS/MS product ion profile of a complex-type monosialylated bifucosylated biantennary structure detected as a doubly sodiated, doubly charged species at *m/z* 1401.1893^{2+}. The spectrum is dominated by ions generated from single and multiple loss(es) of nonreducing sugars (Y-type ions) at HexNAc, NeuAc and dHex residues (e.g. from *m/z* 474.22^{1+} to 1967.96^{1+}), thereby providing some key structurally relevant product ions. For example, the Y-type ion at *m/z* 474.22 is consistent with a reducing fucosylated GlcNAc confirming the position of one of the two fucoses at the reducing end (core-fucose). The B-type ion at *m/z* 847.40 corresponds to a sialylated LacNAc antenna, whereas the one observed at *m/z* 660.32 corresponds to a fully methylated nonsialylated fucosylated LacNAc antenna. The absence of specific product ion corresponding to a sialylated fucosylated LacNAc antenna at *m/z* 1021.49 is in good agreement with the knowledge according to which an α2,6-sialyl LacNAc antenna is a poor acceptor of Lewis-building fucosyltransferases (Britten et al. 1998).

The latest example (see Figure 3C) shows the characterization of the major high-mannose N-glycan structure, which is an hexomannosidic structure terminated by a GlcNAcα1, O-phosphate giving signal as a triply sodiated, doubly charged species at *m/z* 1076.9753^{2+}. The product ion profile is complex as a result of single and multiple fragmentations at reducing and nonreducing HexNAc and phosphate unit. The fragment at *m/z* 1893.79 corresponds to the parent ion having lost one labile HexNAc and bearing a non-methylated phosphate group that conserved its two acidic functions free. The mass difference of 124 Da with *m/z* 1769.86 (single Y-type cleavage) is

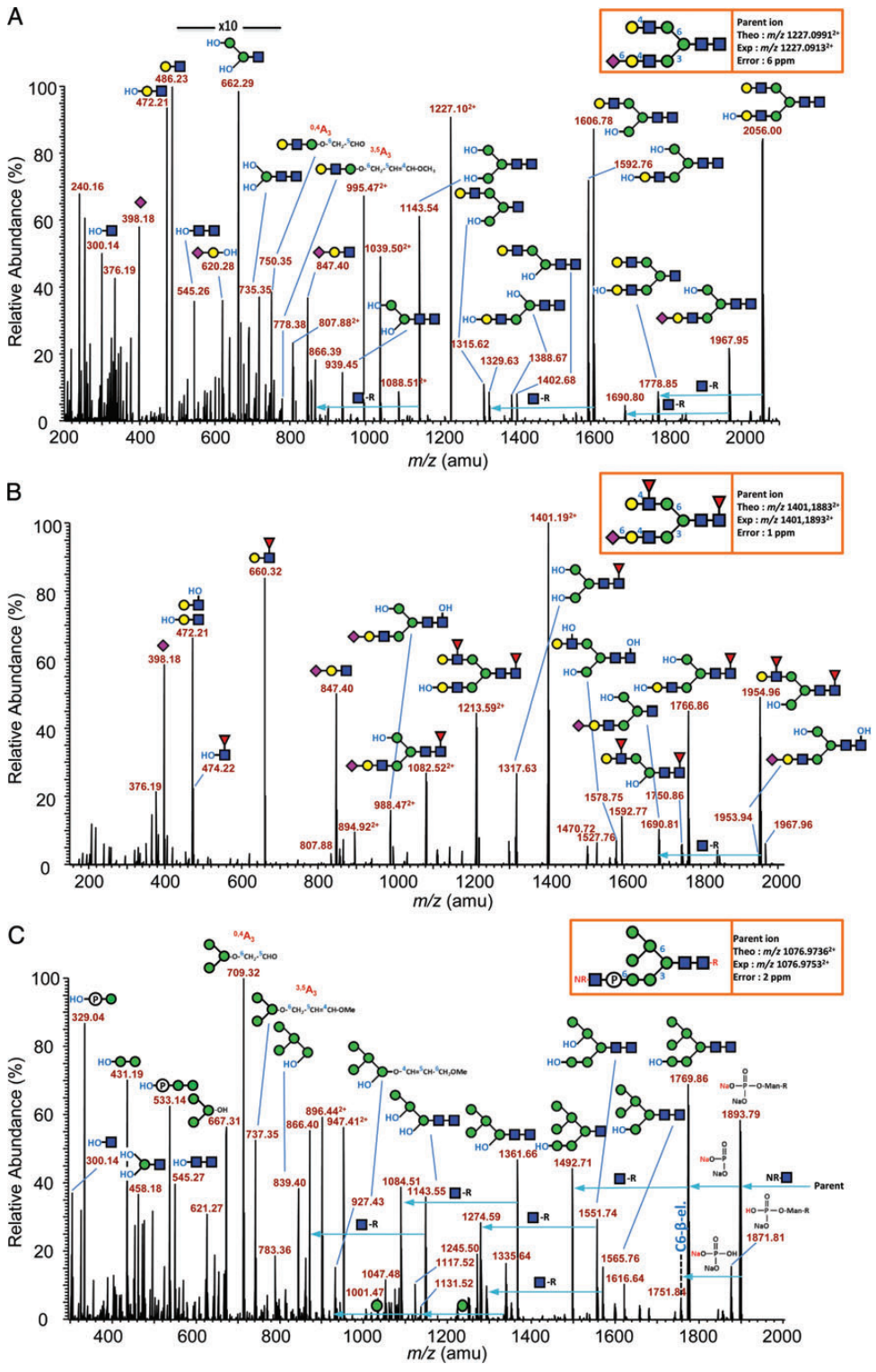

Fig. 3. Positive ion mode nano-ESI-MS/MS sequencing of permethyl rhFVIIa *N*-glycans. (**A**) MS/MS product ion profile of the doubly charged doubly sodiated precursor ion at *m*/*z* 1227.0913, corresponding to a monosialylated biantennary (6 ppm mass accuracy) N-glycan; (**B**) MS/MS product ion profile of the doubly charged doubly sodiated precursor ion at *m*/*z* 1401.1893, corresponding to a monosialylated bifucosylated biantennary *N*-glycan (1 ppm mass accuracy); (**C**) MS/MS product ion profile of the doubly charged triply sodiated precursor ion at *m*/*z* 1076.9753 corresponding to the most intense oligomannose structure, i.e. Man_6-P-GlcNAc (2 ppm mass accuracy). The glycan representation was made according to the nomenclature of the "Consortium of Functional Glycomics" (CFG).

consistent with the loss of the non-methylated phosphate group and two sodium ions. The labile HexNAc is thus directly linked to the N-glycan through a phosphodiester bond.

The two most evident structurally relevant cross-ring cleavage ions resulting from the ring split of the core branching β-Man abundantly detected at *m/z* 709.32 (Man_3-O-CH_2-CHO; ^{0,4}A-type ion) and 737.35 (Man_3–O–CH_2–CH=CH–O–CH3; ^{3,5}A-type ion) are diagnostic ions of the presence of a fully methylated trimannose unit linked to the Manα1,6 arm. This result indicates that the structure composed of a HexNAc-O-phosphate, borne by the Manα1,3 arm, should be the prevalent one. Finally, the presence of B-type product ions at *m/z* 329.04 ($HNaPO_3$-Man) and 533.14 ($HNaPO_3$-Man_2) corresponding respectively to fully methylated mono- and di-mannose units linked to the non-methylated phosphate group and the absence of their mono-hydroxylated counterparts demonstrates that the phosphate group is borne by a terminating Man rather than an internal one. These results do not exclude, however, other minor isomer structures as evidenced from HILIC data. A summary of the proposed structures accompanied by their relative abundance and HILIC RTs is provided in Figure 4.

O-glycosylation investigation by MS and MS/MS of the tryptic peptide [Leu_{39}-Lys_{62}]

Human pd-FVII possesses two O-glycosylation sites located at Ser_{52} and Ser_{60}. Using MS/MS analysis on the tryptic peptide [Leu_{39}-Lys_{62}], Ser_{52} and Ser_{60} have been previously described to bear O-glucose-$(xylose)_{0,\ 1,\ 2}$ and O-fucose motifs, respectively (Fenaille et al. 2008). By using the same methodology, the O-glycosylation state of the present rhFVIIa has been investigated. Figure 5A shows the MS profile of peptide [Leu_{39}-Lys_{62}]. The major signal observed at *m/z* 1011.42 corresponds to the triply charged peptide modified by a fucose and a glucose (theoretical monoisotopic mass of 3031.21 Da vs. an experimental mass of 3031.24 Da). A second signal observed at *m/z* 1099.44 corresponds to the addition of two xyloses, the form with only one xylose being almost absent. A minor signal labeled at *m/z* 962.73 is indicative of a trace of peptide without fucosylation. Figure 5B and C show the MS/MS spectra of parent ions at *m/z* 1099.4 and 1011.4, respectively. Subsequent losses of the labile sugar moieties can be observed and, similar to the Fenaille et al. study, the loss of the glucose is observed only after the previous loss of the two xyloses sugar, confirming the linkage of xylose residues to glucose as observed for pd-FVII. Some minor glycosylated b and y fragment ions indicating O-glucosylation at Ser_{52} and O-fucosylation at Ser_{60} were retrieved (data not shown). Cumulative data obtained during development studies indicated no significant variation of the O-glycosylation profile. For this reason, O-glycosylation was not considered relevant to additional consistency studies.

Sampling strategy for N-glycosylation consistency study

The marketing of a biomolecule produced using transgenic animal raises the question of being able to ensure its long-term stable production. In the particular case of transgenesis, PTMs such as N-glycosylation can be expected to evolve during the time course of lactation as the global composition of the milk (lipid, protein content etc.) is well known to evolve as well (Maertens et al. 2006). Furthermore, the consistency of the N-glycosylation profile has to be demonstrated with the generation

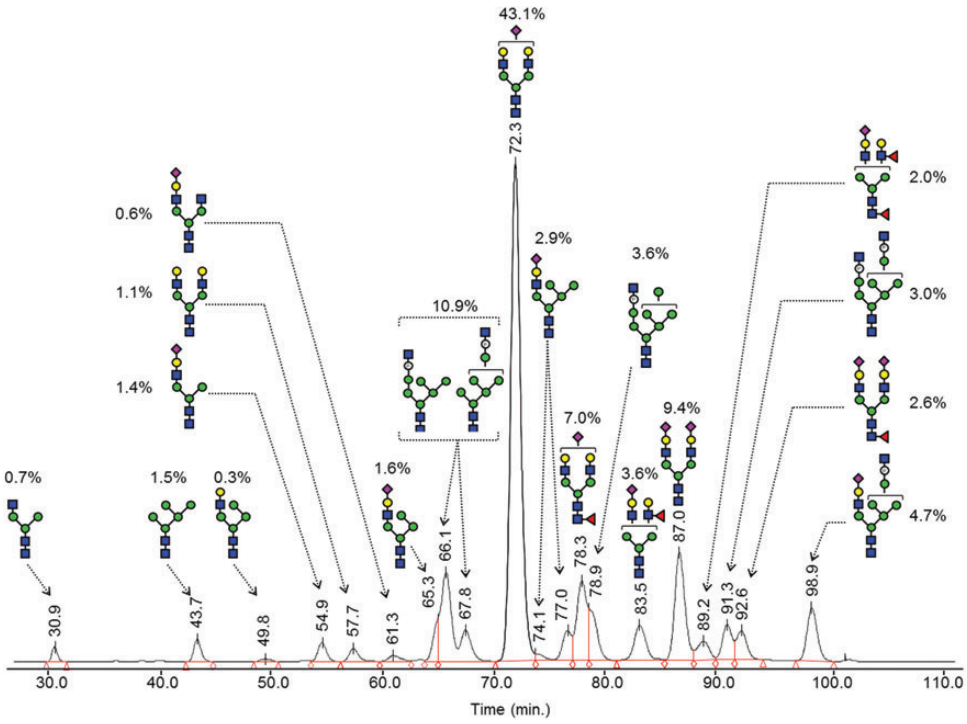

Fig. 4. A summary of identified N-glycan structures of rhFVIIa and quantification from HILIC profiling and MS studies. The glycan representation was made according to the nomenclature of the CFG.

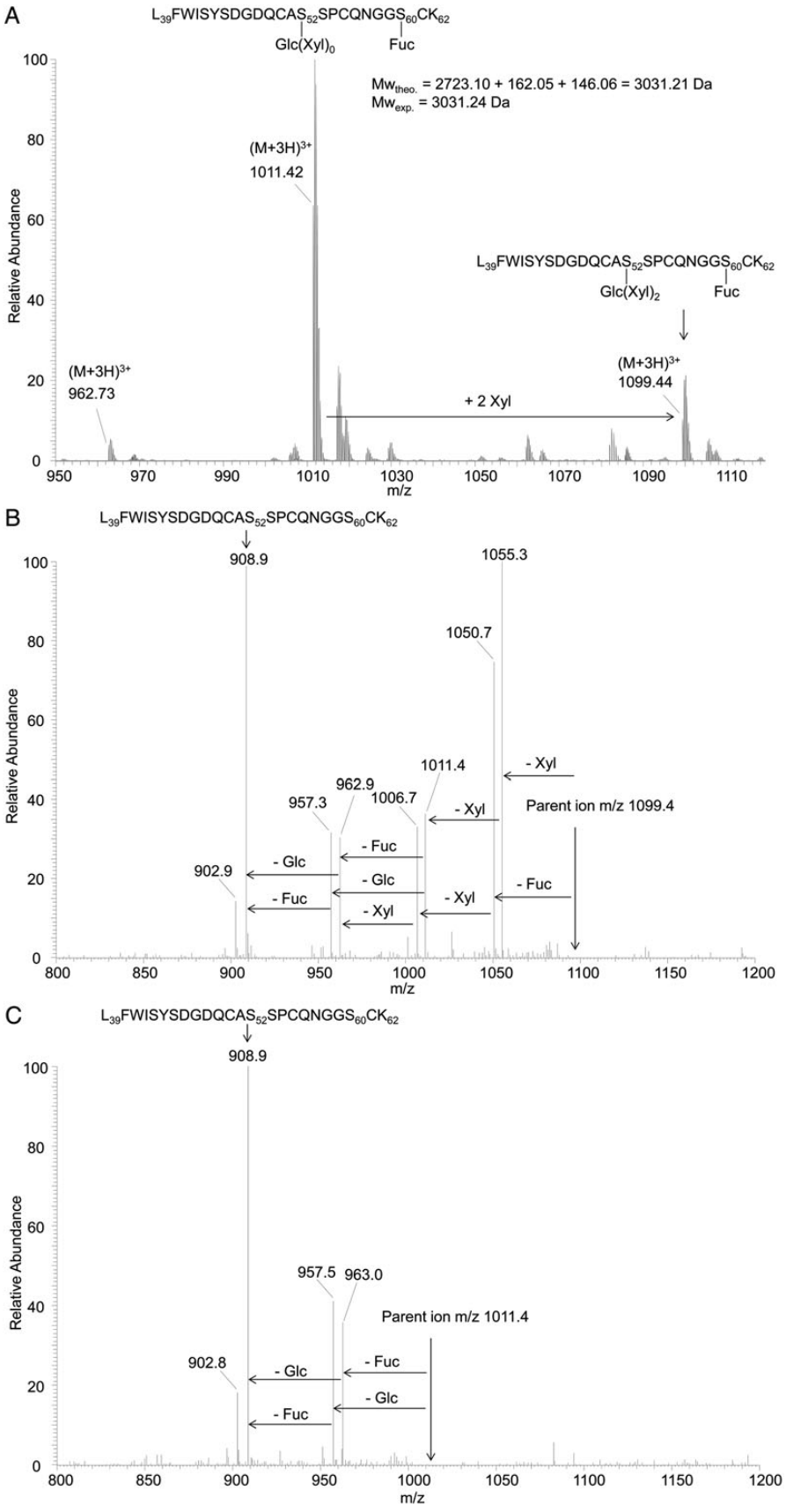

Fig. 5. ESI-MS profile of the tryptic peptide [Leu_{39}-Lys_{62}] (**A**), MS/MS spectrum of *m/z* 1099.4 (**B**) and MS/MS spectrum of *m/z* 1011.4 (**C**).

of new strains of genetically modified animals or during consecutive lactations of the same strain. To achieve a greater production consistency, a uniform rabbit herd has been bred in a reproducible manner. Briefly, rabbit females were programmed to give birth at the same time. Four days after birth, females were milked and selected according to several criteria such as milk volume and rhFVII antigen level to ensure high and constant protein productivity. Milk was then collected from Days 5 to 22. New females (F"x" + 1) were constantly reintroduced into the herd to replace old ones and to ensure a long-term uniform herd, consisting of female rabbits having similar history and productivity.

For glycosylation consistency evaluation, data were collected from homogeneous minipools of six milking females of the same breeding generation, i.e. same founder (F"x"), sharing the same number of lactations (L"x") and during the same lactation period (D"x"). The study of these homogeneous minipools allowed us to evaluate putative variations excluding heterogeneity inherent to individual rabbits. Homogeneous minipools from generations F2, F3, F4, from lactations L1, L2, L5, L6 and over three lactation periods (Days 5, 14 and 22) were generated and used for FVII purification using a single immunoaffinity step (purity > 90% evaluated by SDS–PAGE) to get a final product reflecting the total population secreted in the milk. The N-glycan content of such rhFVIIa purified from the minipools was established using HILIC coupled with fluorescence detection (see Figure 6). Ten representative structures accounting for ~90% of the total pool of glycans were monitored (see Supplementary data, S3) and used as indicators of the consistency, especially for the measurement of fucosylation, sialylation and high-mannose/hybrid levels.

Glycosylation monitoring over successive generation, lactation and during the lactation course

Figure 6 displays the glycan profiles obtained from rhFVIIa purified from the minipools of the study. Two observations can be made: first, the profiles are very similar for a same lactation period, whatever the lactation or generation; secondly, a high content of mono-/bi-sialylated fucosylated structures is observed at an early stage of lactation, whereas these species tend to decrease over the lactation time course. These observations suggest that rhFVIIa production seems reproducible from either lactation to lactation or generation to generation and that most of the variations are observed during the time course of lactation. To investigate in further details, these assumptions, the average percentages and standard deviations (SDs) of sialylated, fucosylated and oligomannose/hybrid structures were calculated for the three lactation time points, using data over several generation/lactation. The results are summarized in Table II. The sialylated structures were found to decrease only very slightly from 78.7% at the beginning of lactation to 75.1% at the end of lactation. The SD of about 1.6–3.7% emphasizes the high level of sialylation reproducibility, which is confirmed by the average of all the data, giving 77.1% of sialylated structures, with only 2.9% SD. The level of fucosylated structures was the highest at the beginning of lactation (38.7%), whereas it was shown to decrease significantly at mid lactation (19.6%) and to increase again at the end of lactation (27.5%). The SDs were observed to decrease during the lactation from 6.8 to 1.5%, which indicates that fucosylation fluctuates at the beginning of lactation whereas it was found to be highly reproducible at middle and end of lactation for various lactations and generations. The overall extent of variation of the fucosylated structures can also be assessed by calculating an SD taking all the samples into account; such calculation gives a result of 9.1% SD. Finally, the level of oligomannose/hybrid structures increased from 14.8% at the beginning of lactation to 17.6% at the end of lactation, which represents only a slight increase during the lactation period. Again, the standard deviation ranging from 1.9 to 2.8% indicates the high reproducibility of this parameter over consecutive generations/lactations. An SD of 2.6% for an average of 16.4% is calculated by using the whole data set, i.e. cumulating variability of lactation, generation and lactation period. This result points out the low variation of these structures during rhFVIIa production. In summary, the sialylated and oligomannose/hybrid structures are consistently produced, even though specific pools of collected milk chosen in distinct conditions are compared. Only the extent of fucosylated structures was found to be variable during the lactation period, with a high variability at the beginning of lactation whatever the considered pools. For a same "advanced" lactation period, the fucose content seems highly reproducible from lactation to lactation or generation to generation. For all the tested samples, the specific activities were similar, at least indicating that fucosylation does not impact the rhFVIIa enzymatic activity.

Pooling strategy and consistency of successive batches

To obtain an homogeneous raw material for the production of batches, milk was always collected and pooled randomly, from the day-to-day production of the herd, hence, avoiding any selective pooling of milk, as for instance from the beginning or the end of a lactation. Approximately 90 rabbit females were milked to provide the raw material necessary for a 150 L-batch size. Figure 7 shows the N-oligosaccharide profiles obtained from consecutive batches obtained at various scales (7.5–150 L) during preclinical development and produced using milk collected from generation F1–F3 and from lactation L2–L5. All the chromatograms can be perfectly overlaid; these data emphasize the perfect batch-to-batch reproducibility of the N-oligosaccharide content and validate the pooling strategy. It is also important to note that the fucose content, shown to be the most important variable at the beginning of lactation and during the lactation period, is now very consistent as a result of averaging the whole milk production.

Discussion

The aim of this study was to address the N-/O-glycan content of a new rhFVIIa produced in the mammary gland of transgenic rabbits and to evaluate its consistency. Concerning rhFVIIa O-glycosylation, MS analysis showed that Ser_{52} and Ser_{60} are modified, respectively, by O-glucose-$(xylose)_{0,\,1,\,2}$ and O-fucose motifs, similar to pd-FVII. Using MS, MS/MS, high performance liquid chromatography (HPLC) and specific exoglycosidases, a total of 20 N-glycan structures were evidenced and quantified. The N-oligosaccharide content was shown to be of the high-mannose, hybrid and complex type with a prevalence of

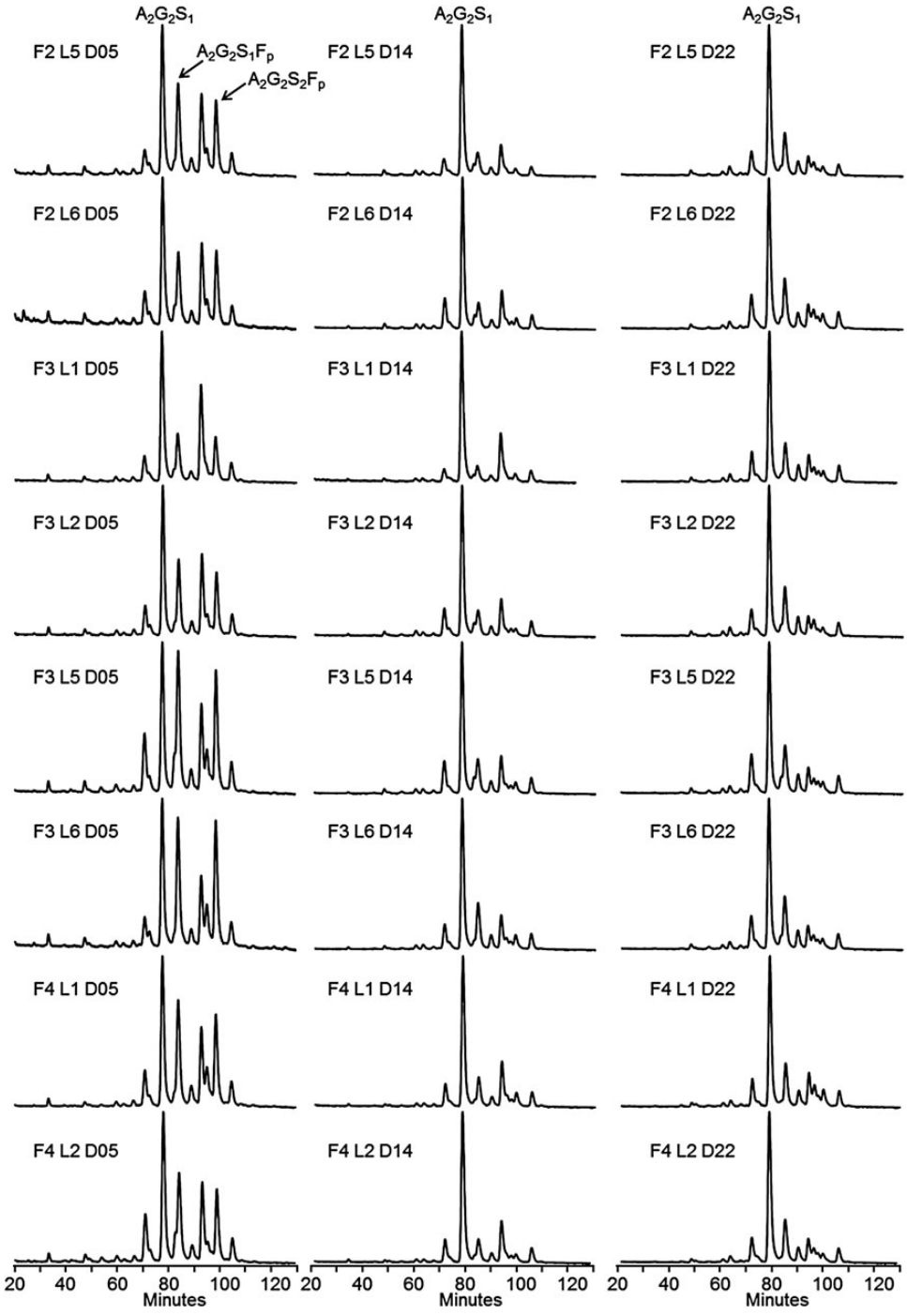

Fig. 6. N-glycan profiles of rhFVIIa on HILIC chromatography after 2-AB labeling of the PNGase F-released N-linked oligosaccharides. Letter F: rabbit funder (generation), L, number of consecutive lactation; D, day of lactation. Twenty-four conditions were screened for N-glycosylation analysis. The major peaks are annotated $A_2G_2S_1$, $A_2G_2S_1F_p$ and $A_2G_2S_2F_p$ on the first chromatogram.

oligomannose/hybrid structures located on the heavy chain of the protein as evidenced by the sensitivity of the heavy chain to Endo-H treatment. This result is in accordance with the fact that an increasing distance of the N-glycosylation site from the C-terminus would lead to a more complex set of N-glycans structures (Bolt et al. 2005; Fenaille et al. 2008). The major oligosaccharides representing 71% of the total pool were of the complex type and composed of biantennary partially sialylated and fucosylated structures (2% neutral, 57% monosialylated and 12% bisialylated). Antennae were shown to be exclusively of Type 2 and sialylated at the α2-6 position like the majority of the glycoproteins produced by the human liver. No antennae

Table II. Average levels of sialylation, fucosylation and oligomannose/hybrid glycans measured over three lactation times with cumulated data from different generation and lactation

Average % of sialylated structures		SD
D05	78.7	1.6
D14	77.4	3.7
D22	75.1	2.0
Total	77.1	2.9
Average % of fucosylated structures		SD
D05	38.7	6.8
D14	19.6	3.5
D22	27.5	1.5
Total	28.6	9.1
Average % of oligomannose/hybrid structures		SD
D05	14.8	2.2
D14	16.8	2.8
D22	17.6	1.9
Total	16.4	2.6

The level of sialylation is expressed as a % of sialylated antenna; the level of fucosylation is expressed as the ratio (%) of fucosylated structures vs. the total content; the level of high-mannose/hybrid is expressed as the ratio (%) of these structures vs. the total content.

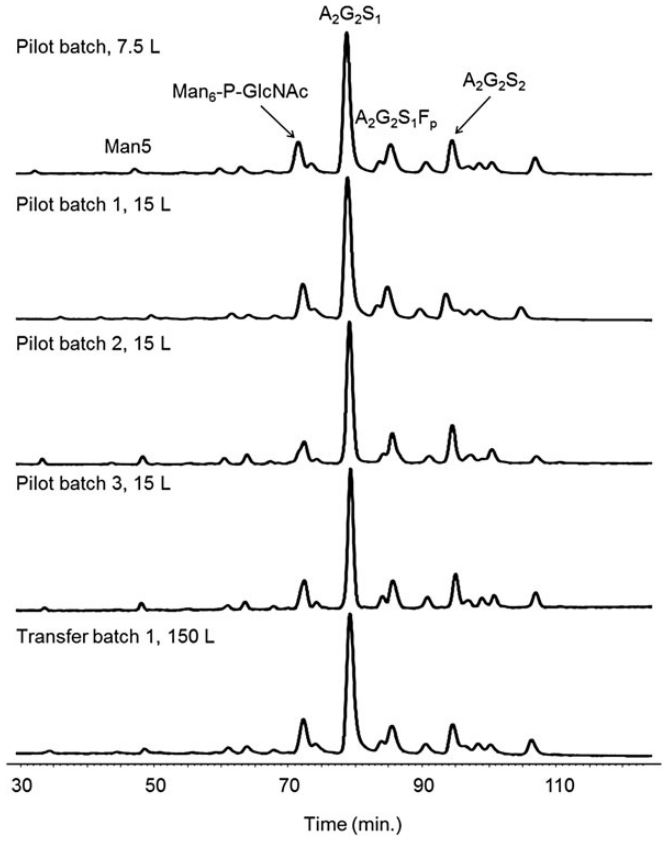

Fig. 7. Consistency of the HILIC N-glycan profiles of five consecutives rhFVIIa batches obtained at different scales (7.5–150 L). The major peak corresponds to a complex biantennary monosialylated N-glycan ($A_2G_2S_1$).

containing either GalNAcβ1-4GlcNAc or Galα1-3Gal epitopes were evidenced after MS/MS fragmentation of the 2-AB and permethyl derivatives. The biantennary monosialylated glycan ($A_2G_2S_1$) is by far the most abundant structure (43.1%) and confers a highly homogeneous glycosylation to the product. Neither tri- nor tetra-antennary structures were detected in this study. Two structures containing a Lewis-X epitope were detected and accounted for ~6% of the total pool. The rest of the glycan pool (29%) was composed of high-mannose and hybrid structures, the major ones being phosphorylated and capped by a terminal GlcNAc group, constituting a GlcNAcα1,O-phosphate motif 6-O-linked to a mannose residue.

Plasma-derived hFVII displays a glycan content composed exclusively of bi- and tri-antennary fully sialylated complex structures (Fenaille et al. 2008). These structures were partially fucosylated and the presence of Lewis-X epitopes was demonstrated. BHK-derived rhFVIIa (NovoSeven®, Novo Nordisk A/S, Bagsvaerd, Denmark) displays a similar glycosylation (Klausen et al. 1998) composed of complex structures. However, it differs by the presence of GalNAcβ1-4GlcNAc motifs described to reduce the half-life of the protein by binding tightly to asialo-glycoprotein receptors (ASGP-Rs) which are involved in the clearance of plasma proteins (Klausen et al. 1998; Park et al. 2003). Undersialylated structures are also well known to bind to ASGP-Rs to mediate protein clearance; however, this phenomenon is predominant with tri- or tetra-antennary undersialylated structures (Chiu et al. 1994; Rice et al. 1995). In the case of the transgenic rhFVIIa, only complex structures of the biantennary type were found, suggesting a minimal effect from uncapped antennae. However, oligomannosidic/hybrid structures that may facilitate clearance through binding to mannose receptor-related C-type lectin receptors (Sorensen et al. 2012) were also detected.

Presently, the glycosylation profiles of rhC1INH and human acid α-glucosidase (rhAGLU) produced in the mammary glands of transgenic rabbits have been detailed in the literature (Koles et al. 2004a; Jongen et al. 2007). Both transgenic proteins have been shown to exhibit conventional "human like" oligomannose-, hybrid- and complex-type structures. Epitopes that may lead to immune reactions in humans, such as Galα1,3Gal and NeuGc antigens, were not detected or present only in trace amounts in the case of NeuGc. The major difference between these two proteins was the presence of capped phosphate groups Man-6-P-1-GlcNAc on some oligomannose- and hybrid-type structures of the rhAGLU lysosomal enzyme. Mannose 6-phosphorylation (Man-6-P) is rather described in the literature for N-glycosylation of lysosomal enzyme (Reitman and Kornfeld 1981a, b; Waheed et al. 1982), however, this epitope was also retrieved in the present transgenic rhFVIIa. To our knowledge, this is only the second description of such a Man-6-(GlcNAcα1,O-)phosphate motif on N-glycans derived from nonlysosomal enzymes, the first one having been published by Nimtz et al. (1995) on human erythropoietin produced by BHK-21 cells. After an in-depth analysis of NovoSeven® glycosylation (data not shown), it was found that at least two structures (Man_6-P-GlcNAc and Man_6-P-GlcNAc-A1S1F) bearing this Man-6-(GlcNAcα1,O-)phosphate motif were present in low abundance (<1%). This result suggests that this epitope may not be that rare among recombinant proteins, but requires analytical techniques sensitive enough to detect it. Advantageously, GalNAcβ1-4GlcNAc epitopes were retrieved neither in rhFVIIa nor in rhC1inh and

rhAGLU produced by transgenic rabbits, whereas, this type of antenna has been largely detected in transgenic proteins produced by goats with rhEPO (Montesino et al. 2008) and rhATIII (Edmunds et al. 1998), pigs with rhFIX (Gil et al. 2008) and cows with rhLF (Yu et al. 2010). Considering that glycosylation is influenced by both the protein sequence and the host cell or animal used for production, the absence of GalNAcβ1,4GlcNAc epitopes on these three distinct proteins produced in rabbit milk suggests that this kind of bioreactor is advantageous, at least for production of proteins with appropriate glycosylation and bioavailability.

After having generated a herd of animals giving similar productivity, we investigated the ability of transgenic rabbits to provide a rhFVIIa with consistent N-glycosylation. Inter-animal variability has been excluded by the constitution of homogeneous minipools. The effects of consecutive lactations, generations as well as the time course of lactation were specifically evaluated. Changes of glycosylation patterns during the time course of lactation were predominantly evidenced. The level of sialylated structures was shown to decrease only slightly during the lactation course. In consequence, no reduction of the timeframe for milk collection was necessary to avoid the collection of an undersialylated product. The very low SD calculated with all the data attests that sialylation is remarkably reproducible whatever the milk pool. A decrease in sialylation or an increase in the protein isoelectric point during the time course of lactation has been previously observed for different mammals (Aoki et al. 1994; Landberg et al. 2000) and was suggested to be a general trend followed by proteins produced in the mammary gland (Koles et al. 2004b). This observation can be explained by a number of influencing biochemical factors, i.e. the availability of sialyltransferase and respective co-factors, the biochemical properties of the protein or the protein expression level. In the case of rhFVIIa, the same downward trend was observed but in moderate proportion, which is an important point as sialylation is known to influence the pharmacokinetic properties of proteins.

In our study, the monitored oligomannose/hybrid structures evolved according to a slight upward trend during the whole lactation period. The low SD obtained, considering all the constituted minipools, confirms that the amount of these structures is stable over successive generations and lactations. This indicates that the current strategy used to manufacture rhFVIIa enables a stable and controlled final proportion of these structures. Considering this point, our results differ from those observed with rhC1INH, where a strong decrease of the oligomannose structures was observed during lactation (Koles et al. 2004b). In this case, the level of oligomannose structures was also correlated with the antigen expression level, especially at the end of lactation. Contrary to the sialylation level that seems to follow a general trend, the evolution of the oligomannose/hybrid content should be more protein dependant. Moreover, it should also be pointed out that the expression level of the rhFVIIa antigen in milk is ~40 times less than that of rhC1INH, which indicates that the glycosylation machinery of the mammary epithelial cells may be differently challenged. Finally, our study shows that the level of fucosylated structures was the highest at the beginning of lactation, with a high SD indicating some variations at the beginning of lactation. The fucosylation level evolved during the lactation time course with a decrease on Day 15 and a later increase on Day 22, with lower SDs indicating an increase of reproducibility toward the end of lactation. The observation of a higher fucosylation level at the beginning of lactation has also been observed for rhC1INH (Koles et al. 2004b). Nevertheless, the fucose content was not considered a critical parameter that could impact on the activity or bioavailability of rhFVIIa. In addition, the glycosylation content of several consecutive batches of the transgenic product has been demonstrated to be highly consistent thanks to pooling of milk without any further selection from the whole herd. The final transgenic rhFVIIa product was found to contain an average level of fucosylation approximately similar to pd-FVII (Fenaille et al. 2008), whereas for NovoSeven®, glycan structures were almost completely fucosylated.

The use of this herd of transgenic rabbits provides a new source of consistent bioactive rhFVIIa and presents the advantage of being easily expandable, assuring thus a stable market supply.

Materials and methods

Materials

Bi-α2,3-sialylated biantennary N-glycan ($A_2G_2S_2$) standard, PNGase F-based N-deglycosylation kits, 2-aminobenzamide (2-AB)-labeling and DMB-labeling kits were purchased from Europa Bioproducts (Cambridge, England). Flavobacterium meningosepticum PNGase F, Streptococcus pneumoniae (β1,4)-galactosidase were from Prozyme (San Leandro, CA). *Macrobdella decora* (α2,3)-neuraminidase and trifluoroacetic acid (TFA) were from Merck Biosciences (Darmstadt, Germany). Acetic acid (CH_3COOH), sodium acetate (CH_3COONa), 28–30% (w/w) aqueous ammonium hydroxide (NH_4OH), sodium hydroxide pellets (NaOH), dimethylsulfoxide (DMSO), iodomethane (ICH_3), 1 M sodium cyanoborohydride ($NaBH_3CN$) in tetrahydrofuran (THF), Orbitrap calibration kit, dithiothreitol (DTT), Streptomyces plicatus Endo H and iodoacetamide (IAA) were purchased from Sigma-Aldrich Chemical (St. Louis, MO). 2,5-dihydroxybenzoic acid (DHB) was purchased from Bruker Daltonics (Bremen, Germany). Methanol (MeOH) and acetonitrile (MeCN) were of HPLC reagent grade and purchased from Biosolve (Leenderweg, The Netherland) and JT Baker (Philipsburg, NJ), respectively. All the aqueous solutions were prepared using ultra-pure water (18.2 MΩ cm resistivity at 25°C, total organic carbon (TOC) < 5 ppb). RhFVIIa produced in the milk of transgenic rabbit females and obtained at a purity better than 99% was provided from LFB BIOTECHNOLOGIES® batches currently in development for clinical trials.

Methods

SDS–PAGE profiling of reduced and nonreduced rhFVIIa. The SDS–PAGE was performed under reducing and nonreducing conditions using NuPAGE Novex 4–12% Bis-Tris gels, Xcell SureLock Mini-Cell and the NuPAGE MES running buffer (Invitrogen, Carlsbad, CA). 1 μg of native, PNGase F- and endo H-treated rhFVIIa were loaded into separate wells. The gel-separated rhFVIIa-related bands were revealed by Coomasie Brillant Blue (CBB) staining and the PAGE image was acquired using an ImageScanner III (GE Healthcare, Piscataway, NJ).

The apparent molecular weights were calculated using Quantity One Software (Biorad, Hercules, CA). The N-deglycosylation of rhFVIIa was performed as described below.

N-deglycosylation and purification of the released oligosaccharides. Purified rhFVIIa was desalted by RP-HPLC and lyophilized in aliquots of 200 µg. One aliquot was suspended in 36.5 µL of milliQ water, 10 µL of 5× digestion buffer, 2 µL of denaturing solution and incubated at room temperature for 15 min (kit Prozyme). 0.5 µL of a detergent solution (NP-40) was added to neutralize the excess of sodium dodecyl sulfate (SDS) and 1 µL of a PNGase F solution was finally added (2.5 mU). N-deglycosylation was carried out overnight at 37°C. The glycans were purified by solid-phase extraction (SPE) onto a 50-mg Hypersep porous graphitized carbon (hypercarb) column (Thermo Fischer Scientific, Bremen, Germany) (Packer et al. 1998). The SPE column was sequentially washed with 1 mL methanol and 2 × 1 mL of a 0.1% (v/v) aqueous TFA. The oligosaccharides were dissolved in 200 µL of a 0.1% (v/v) aqueous TFA, applied to the column and washed with 2 × 1 mL of a 0.1% (v/v) aqueous TFA. The elution of the glycans was performed by applying 2 × 500 µL of a 25% (v/v) aqueous MeCN containing 0.1% (v/v) TFA. The eluate was vacuum-dried.

Fluorescence labeling of N-glycans by reductive amination with 2-aminobenzamide. 2-AB and $NaBH_3CN$ were reconstituted in DMSO/acetic acid (7:3, v/v) to give concentrations of 0.35 and 1 M, respectively. Labeling was performed by adding 10 µL of the labeling solution to the pool of dried glycans corresponding to 200 µg of total protein. The reaction was kept at a temperature of 37°C for 18 h (overnight) to avoid loss of sialic acids that can occur with higher temperatures. The excess reagent was removed by SPE Oasis® HLB cartridges (Waters, Milford, MA). The cartridge was washed and wetted by 2 × 1 mL of MeCN. The labeled oligosaccharides were diluted in 200 µL of MeCN, applied to the cartridge and washed with 2 × 200 µL of MeCN. The elution of the glycans was performed by applying 2 × 500 µL of a 20% (v/v) aqueous MeCN. The eluate was vacuum-dried.

Permethylation of the released oligosaccharides. The dried glycans were subjected to permethylation according to Ciucanu and Kerek's procedure with some modifications (Ciucanu et Kerek, 1984). Briefly, the samples were dissolved into 100 µL of NaOH slurry at 200 mg/mL in DMSO containing a maximum of 2% (v/v) trace of water and were vigorously stirred for 10 min at room temperature. 100 µL of methyl iodide was then added, and the samples were vigorously stirred for 2 h at room temperature, with additional adding of 100 µL of methyl iodide after 30 min. The reaction was stopped by first evaporating the excess methylating reagent under a stream of compressed air for 30 min and then by recovering the samples with 100 µL of cold 25% (v/v) aqueous acetic acid. Diiodine, formed during permethylation, which can disturb further mass spectrometric analyses, was removed by addition of an excess of sodium thiosulfate to samples prior to the SPE sample clean-up. The permethyl oligosaccharides were desalted onto a 50 mg Hypersep silica-based reversed-phase (C18) SPE column (Thermo Fischer Scientific, Bremen, Germany), which was wetted beforehand and equilibrated using 1 mL of methanol and 2 × 1 mL of a 3% (v/v) aqueous MeCN, respectively. The bound material was washed using 2 × 1 mL of a 3% (v/v) aqueous MeCN followed by 1 mL of a 10% (v/v) aqueous MeCN, and the elution was conducted by the application of 2 × 500 µL of an 80% (v/v) aqueous MeCN. The eluate was then vacuum-dried.

Sialic-acid profiling. 10–20 µg of vacuum-dried rhFVII were submitted to a chemical desialylation in the presence of 2-M aqueous acetic acid for 3 h at 80°C. The reaction was stopped by adding three volumes of cold ethanol followed by incubation at 4°C for 15 min, and the protein material was then centrifuged at 10,000 g for 10 min at 4°C. The sialic-acid-containing supernatant was vacuum-dried. Sialic acids were recovered in 5 µL of derivatization reagent consisting of 7 mM 1,2-diamino-4,5-methylène-dioxybenzene, 18 mM sodium dithionite, 0.75 M β-mercaptoethanol and 1.4 M acetic acid, and the reaction conducted at 50°C for 3 h in the dark. The reaction was stopped by a 100-fold dilution with ultra-pure water. The derivatives were separated by reversed-phase HPLC onto a 150-mm length × 2.1 mm ID silica-bonded C18 Uptisphere® column (Interchim, Montluçon, France), equilibrated at 30°C in acetonitrile/methanol/eau (9:7:84; v/v/v). The elution products were monitored at $\lambda_{exc.} = 373$ nm/$\lambda_{ém.} = 448$ nm using a fluorimetric detector RF-10A XL (Shimadzu, Kyoto, Japan). The separation was carried out by an isocratic elution at 0.1 mL/min, à 30°C for 1 h.

Hydrophilic interaction chromatography. Dried 2-AB-labeled glycans were recovered in acetonitrile/water (96:4; v/v) and analyzed following two distinct protocols differing by column formats and detections used, i.e. using a classical normal-bore column for fluorescence detection and using a capillary column for both fluorescence and mass spectrometry detections. For both configurations, ammonium formate 50 mM, pH 4.4, and absolute acetonitrile were, respectively, used as Buffer A and Buffer B.

Normal-bore configuration: The separation was carried out using a GOLD HPLC system (Beckman Coulter, Fullerton, CA). The HILIC column was of the TSK-gel Amide-80® type (250 × 4.6 mm, 5 µm, 80 Å; Tosoh Biosciences, Stuttgart, Germany) operating at a flow rate of 1 mL/min and equilibrated with 80% B at a temperature of 30°C. The gradient used for analysis was the following: 80–70% B in 15 min, from 70 to 55% B in 150 min and from 55% B to 42% B in 13 min. The column was then washed with 10% B and equilibrated again with 80% B for at least 45 min. The detection was performed by fluorescence $\lambda_{exc.} = 330$ nm/$\lambda_{em.} = 420$ nm on a RF-10A XL fluorimeter (Shimadzu, Duisburg, Germany).

Capillary configuration: The separation was carried out using a U3000 HPLC system fitted with an active nanoflow splitter (Dionex, Sunnyvale, CA). The HILIC column was of the Amide-80 type (250 × 0.3 mm, 5 µm, 80 Å; Grace Alltech, Deerfield, IL) operating at a flow rate of 5 µL/min at a temperature of 50°C and coupled to a preconcentration column packed with the same phase (10 × 0.3 mm, 5 µm, 80 Å; Grace Alltech, Deerfield, IL) operating at a flow rate of 50 µL/min. Glycans were loaded onto the preconcentration column at 80% of B

during 5 min and submitted to the gradient of the analytical column by the use of a 12-position valve switch. The gradient used for analysis was the following: 0 min, 80% B; 5 min, 68% B; 100 min, 58% B. The column was then washed with 20% B and equilibrated again with 80% B for at least 45 min. Fluorescence detection was performed using a 325-nm Laser Induce Fluorescence (LIF) detector (Zetalif™ Discovery; Picometrics™, Ramonville, France). MS detection was carried out, using an linear trap quadrupole (LTQ)-Orbitrap hybrid mass spectrometer (Thermo Fischer Scientific, Bremen, Germany), in the positive ESI ion mode and using the following parameters: spray voltage of 4.6 kV; capillary voltage of 47 V; tube lens voltage of 180 V and temperature set at 180°C. External calibration was performed using the manufacturer's calibration mix, giving rise to a mass accuracy better than 5 ppm. Survey full-scan MS spectra were acquired in the Orbitrap analyzer from *m*/*z* 750 to 4000 at a resolving power of 30,000 (*m*/*z* 400 amu) and using an automated gain control (AGC) target value set to 1×10^6 charges with a maximum fill time of 1 s. MS/MS spectra were generated in the data-dependent mode by collision-induced dissociation of the most intense molecular ion within the LTQ, using a five-amu isolation width and normalized collision energy of 30%. Fragments were analyzed in the Orbitrap analyzer at a resolving power of 7500 (*m*/*z* 400 amu). The cap-liquid chromatography (LC) and LIF systems were driven by the Thermofisher Scientific Xcalibur™ software. Interpretations of MS/MS spectra as well as the calculation of the theoretical masses were assisted by the Glycoworkbench™ software (EUROCarbDB, www.eurocarbdb.org).

Enzymatic α2,3-desialylation. An aliquot of the purified 2-AB-labeled N-glycans was first reconstituted in a 125-mM sodium phosphate buffer, pH 5.5, and incubated overnight at 37°C with 140 mU/μL of α2,3-neuraminidase (EC 3.2.1.18). The digestion efficiency was assessed by using 2 μg of a pure bi-α2,3-sialylated biantennary N-glycan ($A_2G_2S_2$) standard as a control. The exoglycosidase was next removed by a cold alcoholic precipitation, and the supernatant containing the digested products was vacuum-dried before HILIC analysis.

Nanoelectrospray ionization-tandem mass spectrometry analyses of permethyl oligosaccharides. MS analyses of the permethyl N-glycans were performed using a LTQ-Orbitrap hybrid mass spectrometer fitted with a nano-ESI ion source (Thermo Fischer Scientific, Bremen, Germany) under the control of the Tune Plus 2.4 software. Samples were infused at 20–80 nL/min from a 75% (v/v) aqueous methanol containing 5 mM sodium acetate through a 0.69 μm ID nano-ESI uncoated borosilicate glass emitter tip (New Objectives, Woburn, MA). MS detection was carried out in the positive ion mode with the following parameters: spray voltage of 1.5 kV; capillary voltage of 47 V; tube lens voltage of 150 V and temperature set at 180°C. External calibration was performed using the manufacturer's calibration mix, giving rise to a mass accuracy better than 5 ppm. The survey full-scan MS as well as MS/MS spectra were acquired in the Orbitrap analyzer at a resolving power of 30,000 (at *m*/*z* 400) and using an AGC target value set to 1 E6 charges. HCD was used to fragment the precursor ions of interest using an isolation width of 5 amu and combining low (60–90 eV) and high (110–150 eV) collisional activation energy in order to collect a wide range of structurally relevant product ions such as those derived from cross-ring cleavages (Domon and Costello 1988).

MALDI-TOF analyses of the permethyl oligosaccharides. MALDI MS and MS/MS experiments were performed on an Autoflex II instrument (Bruker Daltonics, Bremen, Germany) using the Flex Control 2.5 software. The desorption as well as the laser-induced dissociation of the molecular ions were carried out by a nitrogen laser irradiating at a frequency of 50 Hz and at 20–30% and 40–70% of maximum laser power, respectively. In MS, the mass spectrometer was operated in either positive or negative reflectron ion mode by delayed extraction with an accelerating voltage of 25 kV. The pulse delay time was set to 350 ns to obtain the best resolution and mass accuracy for the molecular ions of *m*/*z* comprised between 1000 and 3000 Da. In MS/MS, the accelerating voltage was first set to 8 kV and the precursor ions of interest, accompanied by their in-source-generated daughter ions, were selected using a deflector ion gate. The daughter ions were further reaccelerated at 19 kV within the "lift" cell. All mass spectra recorded represent accumulated mass spectra obtained from 3000 laser shots. The external calibration of the mass spectra was carried out by using the monoisotopic masses of the protonated mixture of standard peptides: bradykinin fragment [1–7] (*m*/*z* 757.400), human angiotensin II (*m*/*z* 1046.542), human angiotensin I (*m*/*z* 1296.685), P substance (*m*/*z* 1347.735), bombesin (*m*/*z* 1619.822), renin (*m*/*z* 1758.933) and two adrenocorticotropic hormone fragments [1–17] (*m*/*z* 2093.087)/[18–39] (*m*/*z* 2465.199). Positive ion mode experiments were performed by spotting 0.5 μL of a matrix solution (10 mg/mL DHB in a 50% (v/v) aqueous methanol containing 10 mM sodium acetate) onto a polished stainless steel MALDI sample plate and mixed with 0.5 μL of permethyl oligosaccharide solution (dissolved in a 50% (v/v) aqueous methanol) and allowed to vacuum-dry. Concerning the negative ion mode MALDI MS fingerprinting, the matrix solution was also a DHB aqueous solution but without doping with sodium acetate to prevent any ion suppression of negatively charged species.

ESI-MS and MS/MS analysis of O-glycosylated [Leu_{39}-Lys_{62}] peptide. Hundred micrograms of lyophilized rhFVIIa were dissolved in 50 μL of 8 M urea, 0.4 M ammonium bicarbonate solution, pH 8.0. Disulfide bridge reduction was accomplished by adding 10 μL of a 100 mM DTT solution in water and incubating the resulting mixture for 15 min at 55°C. After cooling at room temperature, 10 μL of a 200 mM IAA solution in water was added and the solution was incubated at RT for 30 min in the dark. After an eightfold dilution with water, digestion with trypsin (1:25, w/w) was performed overnight at 37°C. The peptides obtained after digestion were injected on an Acclaim® PepMap100 C18 column (0.75 × 150 mm, 3 μm), using a U3000 nano-LC system fitted with a preconcentration setup and interfaced with a high-resolution LTQ-Orbitrap mass spectrometer (Thermofischer Scientific™, Bremen, Germany) operating in the positive ion mode. The nanospray was obtained with the application of a 1.5-kV capillary voltage. The

survey full-scan MS was acquired in the Orbitrap analyzer at a resolving power of 30,000 (at *m*/*z* 400) and using an AGC target value set to 1 E6 charges, whereas top five MS/MS spectra were acquired in the trap analyzer using CID fragmentation mode and AGC target value to 2 E4 charges.

Supplementary data

Supplementary data for this article is available online at http://glycob.oxfordjournals.org/.

Funding

This work was supported by LFB Biotechnologies.

Acknowledgements

The authors thank all colleagues at rEVO Biologics for their contribution to the recombinant human FVIIa project.

Conflict of interest

All the authors are employees of LFB Biotechnologies Company, currently developing a new rhFVIIa product presently described in this manuscript.

Abbreviations

2-AB, 2-aminobenzamide; AGC, automated gain control; ASGP-Rs, asialo-glycoprotein receptors; BHK, baby hamster kidney; CFG, Consortium of Functional Glycomic; DMB, 1,2-diamino-4,5-methylenedioxybenzene; DMSO, dimethylsulfoxide; DTT, dithiothreitol; EndoH, endo-β-N-acetylglucosaminidase H digestion; HCD, high-energy collisional dissociation; HILIC, hydrophilic interaction liquid chromatography; IAA, iodoacetamide; LIF, laser induce fluorescence; MALDI, matrix assisted laser desorption ionisation; Man, mannose; Man-6-P, Mannose 6-phosphorylation; MS, mass spectrometry; nano-ESI, nanoelectrospray ionization; NeuAc, N-acetylneuraminic acid; NeuGc, N-glycolylneuraminic acid; PNGase F, peptide-N_4-(N-acetyl-beta-glucosaminyl)asparagine amidase; PTMs, post-translational modifications; rhAGLU, human acid α-glucosidase; rhC1INH, human C1 inhibitor; RT, retention time; SD, standard deviations; SDS–PAGE, sodium dodecyl sulfate–polyacrylamide gel electrophoresis; SPE, solid-phase extraction; TFA, trifluoroacetic acid.

References

Aoki N, Ujita M, Kuroda H, Urabe M, Noda A, Adachil T, Nakamura R, Matsuda T. 1994. Immunologically cross-reactive 57 kDa and 53 kDa glycoprotein antigens of bovine milk fat globule membrane: Isoforms with different N-linked sugar chains and differential glycosylation at early stages of lactation. *Biochim Biophys Acta*. 1200:227–234.

Bolt G, Kristensen C, Steenstrup TD. 2005. Posttranslational N-glycosylation takes place during the normal processing of human coagulation factor VII. *Glycobiology*. 15:541–547.

Brinkhous KM, Hedner U, Garris JB, Diness V, Read MS. 1989. Effect of recombinant factor VIIa on the hemostatic defect in dogs with hemophilia A, hemophilia B, and von Willebrand disease. *Proc Natl Acad Sci USA*. 86:1382–1386.

Britten CJ, van den Eijnden DH, McDowell W, Kelly VA, Witham SJ, Edbrooke MR, Bird MI, de Vries T, Smithers N. 1998. Acceptor specificity of the human leukocyte alpha3 fucosyltransferase: Role of FucT-VII in the generation of selectin ligands. *Glycobiology*. 8:321–327.

Carugati A, Pappalardo E, Zingale LC, Cicardi M. 2001. C1-inhibitor deficiency and angioedema. *Mol Immunol*. 38:161–173.

Chiu MH, Tamura T, Wadhwa MS, Rice KG. 1994. In vivo targeting function of N-linked oligosaccharides with terminating galactose and N-acetylgalactosamine residues. *J Biol Chem*. 269:16195–16202.

Ciucanu I, Kerek F. 1984. A simple and rapid method for the permethylation of carbohydrates. *Carbohydr Res*. 131:209–217.

Domon B, Costello CE. 1988. Structure elucidation of glycosphingolipids and gangliosides using high-performance tandem mass spectrometry. *Biochemistry*. 27:1534–1543.

Edmunds T, Van Patten SM, Pollock J, Hanson E, Bernasconi R, Higgins E, Manavalan P, Ziomek C, Meade H, McPherson JM, et al. 1998. Transgenically produced human antithrombin: Structural and functional comparison to human plasma-derived antithrombin. *Blood*. 91:4561–4571.

Fenaille F, Groseil C, Ramon C, Riande S, Siret L, Chtourou S, Bihoreau N. 2008. Mass spectrometric characterization of N- and O-glycans of plasma-derived coagulation factor VII. *Glycoconj J*. 25:827–842.

Gil GC, Velander WH, Van Cott KE. 2008. Analysis of the N-glycans of recombinant human Factor IX purified from transgenic pig milk. *Glycobiology*. 18:526–539.

Hansson K, Stenflo J. 2005. Post-translational modifications in proteins involved in blood coagulation. *J Thromb Haemost*. 3:2633–2648.

Hedner U, Lee CA. 2011. First 20 years with recombinant FVIIa (NovoSeven). *Haemophilia*. 17:e172–e182.

Jongen SP, Gerwig GJ, Leeflang BR, Koles K, Mannesse ML, van Berkel PH, Pieper FR, Kroos MA, Reuser AJ, Zhou Q, et al. 2007. N-glycans of recombinant human acid alpha-glucosidase expressed in the milk of transgenic rabbits. *Glycobiology*. 17:600–619.

Joziasse DH, Schiphorst WE, van den Eijnden DH, van Kuik JA, van Halbeek H, Vliegenthart JF. 1985. Branch specificity of bovine colostrum CMP-sialic acid: N-acetyllactosaminide alpha 2—6-sialyltransferase. Interaction with biantennary oligosaccharides and glycopeptides of N-glycosylproteins. *J Biol Chem*. 260:714–719.

Kamerling JP, Boons G-J. 2007. *Comprehensive Glycoscience: From Chemistry to Systems Biology*. 1st ed. Amsterdam; Boston: Elsevier.

Klausen NK, Bayne S, Palm L. 1998. Analysis of the site-specific asparagine-linked glycosylation of recombinant human coagulation factor VIIa by glycosidase digestions, liquid chromatography, and mass spectrometry. *Mol Biotechnol*. 9:195–204.

Koles K, van Berkel PH, Pieper FR, Nuijens JH, Mannesse ML, Vliegenthart JF, Kamerling JP. 2004a. N- and O-glycans of recombinant human C1 inhibitor expressed in the milk of transgenic rabbits. *Glycobiology*. 14:51–64.

Koles K, van Berkel PH, Mannesse ML, Zoetemelk R, Vliegenthart JF, Kamerling JP. 2004b. Influence of lactation parameters on the N-glycosylation of recombinant human C1 inhibitor isolated from the milk of transgenic rabbits. *Glycobiology*. 14:979–986.

Landberg E, Huang Y, Stromqvist M, Mechref Y, Hansson L, Lundblad A, Novotny MV, Pahlsson P. 2000. Changes in glycosylation of human bile-salt-stimulated lipase during lactation. *Arch Biochem Biophys*. 377:246–254.

Lusher J, Ingerslev J, Roberts H, Hedner U. 1998. Clinical experience with recombinant factor VIIa. *Blood Coagul Fibrinolysis*. 9:119–128.

Maertens L, Lebas F, Szendrö Z. 2006. Rabbit milk: A review of quantity, quality and non-dietary affecting factors. *World Rabbit Sci*. 14:205–230.

Menache D, Grossman BJ, Jackson CM. 1992. Antithrombin III: Physiology, deficiency, and replacement therapy. *Transfusion*. 32:580–588.

Montesino R, Toledo JR, Sanchez O, Sanchez A, Harvey DJ, Royle L, Dwek RA, Rudd PM, Gerwig GJ, Kamerling JP, et al. 2008. Monosialylated biantennary N-glycoforms containing GalNAc-GlcNAc antennae predominate when human EPO is expressed in goat milk. *Arch Biochem Biophys*. 470:163–175. Epub 2007 Dec 2005.

Morelle W, Faid V, Michalski JC. 2004. Structural analysis of permethylated oligosaccharides using electrospray ionization quadrupole time-of-flight tandem mass spectrometry and deutero-reduction. *Rapid Commun Mass Spectrom*. 18:2451–2464.

Nimtz M, Wray V, Rudiger A, Conradt HS. 1995. Identification and structural characterization of a mannose-6-phosphate containing oligomannosidic

N-glycan from human erythropoietin secreted by recombinant BHK-21 cells. *FEBS Lett*. 365:203–208.

Packer NH, Lawson MA, Jardine DR, Redmond JW. 1998. A general approach to desalting oligosaccharides released from glycoproteins. *Glycoconj J*. 15:737–747.

Park EI, Manzella SM, Baenziger JU. 2003. Rapid clearance of sialylated glycoproteins by the asialoglycoprotein receptor. *J Biol Chem*. 278:4597–4602.

Reitman ML, Kornfeld S. 1981a. Lysosomal enzyme targeting. N-Acetylglucosaminylphosphotransferase selectively phosphorylates native lysosomal enzymes. *J Biol Chem*. 256:11977–11980.

Reitman ML, Kornfeld S. 1981b. UDP-N-acetylglucosamine:glycoprotein N-acetylglucosamine-1-phosphotransferase. Proposed enzyme for the phosphorylation of the high mannose oligosaccharide units of lysosomal enzymes. *J Biol Chem*. 256:4275–4281.

Rice KG, Chiu MH, Wadhwa MS, Thomas VH, Stubbs HJ. 1995. In vivo targeting function of N-linked oligosaccharides. Pharmacokinetic and biodistribution of N-linked oligosaccharides. *Adv Exp Med Biol*. 376:271–282.

Sorensen AL, Clausen H, Wandall HH. 2012. Carbohydrate clearance receptors in transfusion medicine. *Biochim Biophys Acta*. 1820:1797–1808.

Tomokiyo K, Yano H, Imamura M, Nakano Y, Nakagaki T, Ogata Y, Terano T, Miyamoto S, Funatsu A. 2003. Large-scale production and properties of human plasma-derived activated Factor VII concentrate. *Vox Sang*. 84:54–64.

van Berkel PH, Welling MM, Geerts M, van Veen HA, Ravensbergen B, Salaheddine M, Pauwels EK, Pieper F, Nuijens JH, Nibbering PH. 2002. Large scale production of recombinant human lactoferrin in the milk of transgenic cows. *Nat Biotechnol*. 20:484–487.

Van Cott KE, Velander WH. 1998. Transgenic animals as drug factories: A new source of recombinant protein therapeutics. *Expert Opin Investig Drugs*. 7:1683–1690.

Varki A. 1993. Biological roles of oligosaccharides: All of the theories are correct. *Glycobiology*. 3:97–130.

Vella GJ, Paulsen H, Schachter H. 1984. Control of glycoprotein synthesis. IX. A terminal Man alpha l-3Man beta 1- sequence in the substrate is the minimum requirement for UDP-N-acetyl-D-glucosamine: Alpha-D-mannoside (GlcNAc to Man alpha 1–3) beta 2-N-acetylglucosaminyltransferase I. *Can J Biochem Cell Biol*. 62:409–417.

Viseux N, de Hoffmann E, Domon B. 1997. Structural analysis of permethylated oligosaccharides by electrospray tandem mass spectrometry. *Anal Chem*. 69:3193–3198.

Waheed A, Hasilik A, von Figura K. 1982. UDP-N-acetylglucosamine:lysosomal enzyme precursor N-acetylglucosamine-1-phosphotransferase. Partial purification and characterization of the rat liver Golgi enzyme. *J Biol Chem*. 257:12322–12331.

Yu T, Guo C, Wang J, Hao P, Sui S, Chen X, Zhang R, Wang P, Yu G, Zhang L, et al. 2010. Comprehensive characterization of the site-specific N-glycosylation of wild-type and recombinant human lactoferrin expressed in the milk of transgenic cloned cattle. *Glycobiology*. 21:206–224.